

Cite this: *Chem. Commun.*, 2012, **48**, 11002–11004

www.rsc.org/chemcomm

COMMUNICATION

Fabrication of heterogeneous exposed core–shell catalyst array using the space specificity of an embodied micelle and their application to a high performance photocatalyst†

Jung Hyo Park, Kyung Min Choi, Jung Hoon Choi, Dong Ki Lee, Hyung Joon Jeon, Hu Young Jeong and Jeung Ku Kang*

Received 23rd July 2012, Accepted 25th September 2012

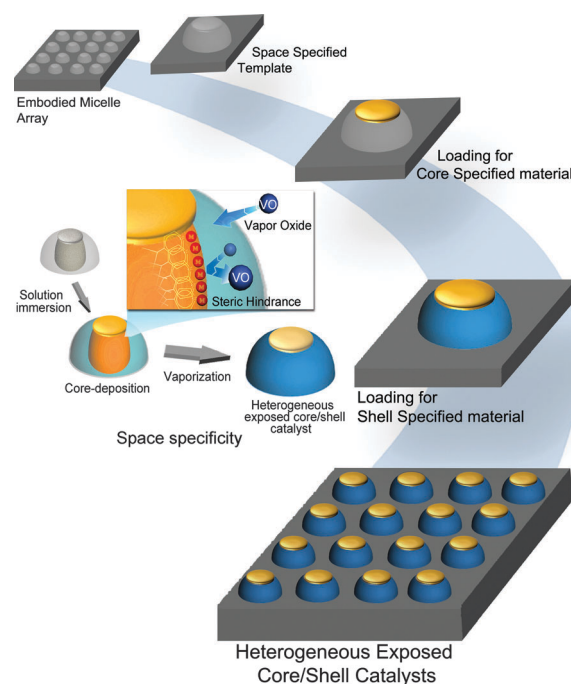
DOI: 10.1039/c2cc36507c

We report a new recipe to synthesize heterogeneous catalyst arrays using the space specificity of an embodied micelle. Also, SEM, AFM, STEM, and TXRF analyses prove that these catalysts are of exposed core–shell types. Furthermore, their structures were found to allow the design of a high performance photocatalyst for water splitting.

Heterogeneous catalysts that exhibit synergistic catalytic effects in a lot of applications have attracted the great attention of many researchers.^{1–4} However, there is no reported method that allows deposition of each catalytic component at the specific position of a heterogeneous catalyst. In this respect, development of heterogeneous catalysts with the space specificity is still state-of-art technology. In the catalytic reactions, most of heterogeneous catalysts are of a powder-type. However, catalysts on a powder-type have their limitations in that dispersion into aqueous media leads to the spontaneous agglomeration giving the rapid decrease of the catalytic activity.^{5–8} Also, thin film-type heterogeneous catalysts have other drawbacks resulting in irregular sizes and random distribution of the co-catalyst components.^{9–12}

In this study, we report a new method to synthesize heterogeneous exposed core–shell catalyst ordered arrays on substrates using embodied micelles (Scheme 1). The micelles have been used as common materials for a thin film process.¹³ In addition, the micelles allow nanoparticles to have a diversity of compositions^{14,15} and can be deposited on various substrates.¹⁶ Due to these advantages of micelles, our strategy to synthesize each core or shell component at the special area of the catalyst uses the space specificity of the embodied micelle. In addition, it is found that this method allows the prevention

of spontaneous agglomeration as well as to enable fabrication of high performance catalysts. The space specificity means that the particular chemical sources are allowed to be deposited selectively at the specific regions of the embodied micelles with the help of a chemical treatment (Fig. S1, ESI†). In this approach, for example, the metal could be deposited in the core region by the solution-immersion process, while the oxide was deposited in the shell region by the vaporization process. The structure at a few nanometer scale sizes and the formation mechanism of these heterogeneous catalysts were unveiled by scanning electron microscopy (SEM), atomic force microscopy (AFM), scanning transmission electron microscopy (STEM), and total X-ray fluorescence (TXRF). This analysis shows that combinations of exposed core and shell components provide a generic method to fabricate different types of



Scheme 1 Representative diagram to synthesize heterogeneous exposed core–shell catalysts using space specificity. The inset diagram shows the principle of space specificity.

Nanocentury KI, Graduate school of EEWS and Department of Materials Science & Engineering, KAIST 373-1 Guseong-Dong, Yuseong Gu, Daejeon, 305-701, Korea. E-mail: jeungku@kaist.ac.kr; Fax: +82-42-350-3310; Tel: +82-42-350-3338

† Electronic supplementary information (ESI) available: The details of fabrication method for the heterogeneous catalysts, the method for evaluation of photocatalytic ability, the formation mechanism of embodied micelles and heterogeneous catalyst, the stability of heterogeneous catalyst for 10 h, and apparent quantum yield equation are provided. See DOI: 10.1039/c2cc36507c

heterogeneous catalyst arrays. In addition, we demonstrate that such heterogeneous catalysts have photocatalytic ability by measuring hydrogen generation and calculating an apparent quantum yield.

First, a micelle solution was prepared by dissolving the diblock copolymer polystyrene-block-poly(4-vinylpyridine) (PS-*b*-P4VP) in toluene to yield a 0.5 wt% solution. The substrate of a silicon wafer was pre-treated by immersion in an ultrasonic bath containing acetone for 10 min followed by drying with a stream of nitrogen. Then, the micelles were spin-coated onto the pre-treated silicon wafer and were found to form a uniformly-sized hexagonal arrangement. The silicon wafer was immersed in methanol at room temperature for 10 h, which led to the embodiment of micelles having distinct core and shell regions (Fig. S1, ESI[†]) for deposition of the catalyst materials on the substrate. Next, metal ions were loaded into the cores of the embodied micelles by submersing the substrate in a 0.1 M methanol solution of the metal precursor for 10 min. After metal ions had been deposited in the core region of the embodied micelles, an oxide material was deposited on the rest of core region in the embodied micelles by vaporization process in the presence of an oxide source inside a sealed chamber at 60 °C for 5 h. We find that microwave plasma-enhanced chemical vapor deposition (MPECVD) removed effectively the micelles used as the template and concurrently reduced the metal ions in the core region of the formed heterogeneous catalyst.

An exposed core is Fe and shell is SiO₂, denoted as Fe-SiO₂, heterogeneous catalyst was synthesized using Fe and Si sources on the scheme described in the above. An SEM image of the produced catalyst (Fig. 1a) shows a lateral distribution of heterogeneous catalysts over a large area with an average size of 25 nm. In the image, distinct core and shell regions of each catalyst particle are seen as a result of the difference in contrast. The contrast difference, attributed to the compositional difference, is also observed in AFM (Fig. 1b) and STEM

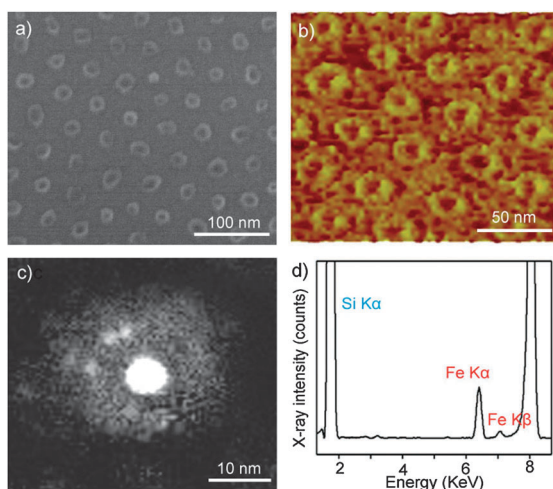


Fig. 1 Structure analysis of a heterogeneous exposed core-shell catalyst array. (a) SEM image showing the structure of the heterogeneous catalyst and its lateral distribution over a large area; (b) AFM tapping mode phase image of the catalyst; (c) ADF STEM image of one particle of the heterogeneous catalyst; (d) Elemental analysis of the catalyst obtained using TXRF.

(Fig. 1c) images. The difference in contrast observed in the AFM tapping mode phase image (Fig. 1b) implies that some compositional changes have occurred. In addition, the structure of a heterogeneous catalyst prepared using the space specificity of the micelles is clearly confirmed by a combination of the annular dark field (ADF) STEM image (Fig. 1c) and the TXRF elemental analysis (Fig. 1d). In STEM images, it should be noted that the metal-containing regions are much brighter than oxide-containing regions.

In addition, we studied the formation mechanism of the heterogeneous exposed core-shell catalysts. In the AFM analysis of micelles (Fig. S1, ESI[†]), the methanol treatment demonstrates that it results in formation of the embodied micelles with the core region of the hydrophilic P4VP units, but with the shell region of the PS units. In addition, the ESI[†] (Fig. S2) clarifies that the oxide materials could be formed only on embodied micelles, while pure metal particles are formed on both pristine and embodied micelles. Also, our ESI[†] (Fig. S1) implies that the chemical treatment by methanol gives the embodied micelles with concave cores. Furthermore, our structural analysis (Fig. S2, ESI[†]) demonstrates that the oxide precursor could not penetrate into the core region of the embodied micelle due to the steric hindrance. However, ionized metal precursors dissolved in solvent can penetrate into the core region of P4VP units by the Lewis acid-base interaction. Consequently, these results demonstrate that this space specificity for metal precursors in the core region allows the formation of heterogeneous exposed core-shell particles. Moreover, the ESI[†] (Fig. S3) proves that the distinct core and shell areas were selectively functionalized with metal ions in the core region and the oxide material in the shell region even for a long oxide vapor deposition time. This implies that metal core particles should not be covered by the oxide materials.

We also fabricated heterogeneous catalysts with other metal and oxide components in the core and shell areas, respectively. Fe and Pt were deposited in the core region, while SiO₂ and TiO₂ were deposited on the shell region. SEM images show the structures of these catalysts and TXRF analyses show the regional distribution of each chemical component (Fig. 2). All the catalysts showed the same type of heterogeneous exposed core-shell structure but with different compositions. In the case of Pt (Fig. 2b and c), SEM images show a high contrast in the core region much brighter than that in oxide shell region. In the case of Pt-TiO₂, we can distinguish Pt and TiO₂ regions by SEM analysis.^{17,18} This is attributed to a higher number of electrons in Pt.

In addition, we determined the efficiency, recyclability, and stability of the heterogeneous catalysts synthesized by our method. In this study, we compared the amount of hydrogen generated from water solution (25 vol% methanol) in the presence of the heterogeneous Pt-TiO₂ catalyst prepared by our method to the amount generated by pure TiO₂ and Pt particles (Fig. 3a), where the amount of hydrogen generated from water solution upon exposure to the ultraviolet light for 3.5 h was analysed by gas chromatography. The amount of hydrogen produced on heterogeneous Pt-TiO₂ catalysts was about 15 mmol m⁻² after 3.5 h, which is much higher than those on other powder-type Pt-TiO₂.^{19,20} In addition,

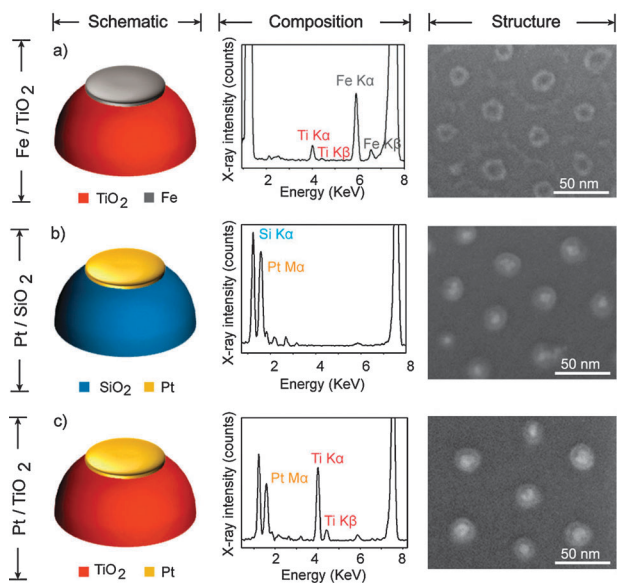


Fig. 2 Structural and compositional analysis (using SEM and TXRF, respectively) of the exposed core-shell heterogeneous catalysts of (a) Fe-TiO₂ (b) Pt-SiO₂ and (c) Pt-TiO₂.

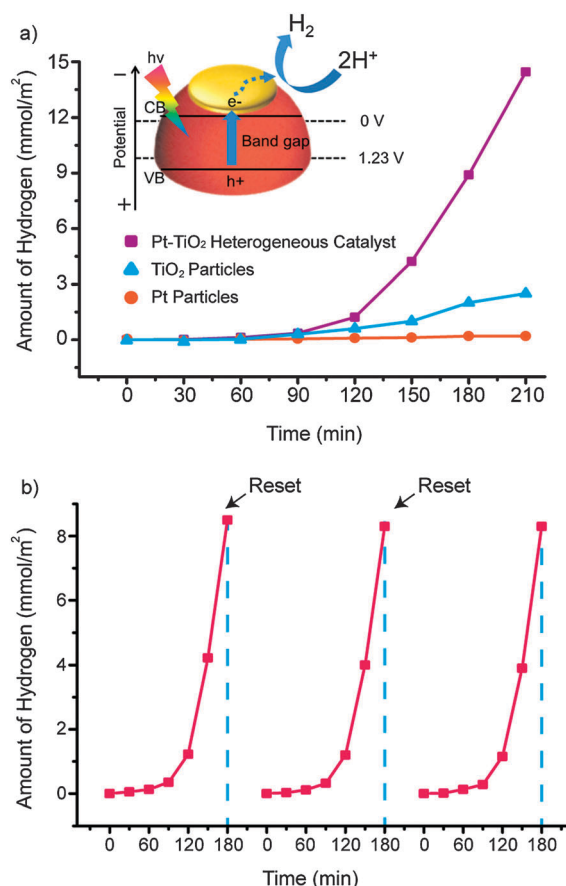


Fig. 3 (a) Hydrogen generation rate by the photocatalytic decomposition of water using heterogeneous Pt-TiO₂, pure TiO₂, and pure Pt catalysts. The inset is the schematic and energy band diagram for the photochemical hydrogen generation from methanol aqueous solution. (b) Recyclability of the heterogeneous Pt-TiO₂ catalyst.

we calculated an apparent quantum yield to determine the photocatalytic ability (see details in eqn (S1), ESI[†]). Furthermore, we conducted recycling experiments of hydrogen generation (Fig. 3b). The reaction was repeated three times and each reaction was continued for 3 h. Prior to each reaction, the gases were evacuated from the reactor and the initial photoreaction conditions were re-established. The results demonstrate that the Pt-TiO₂ catalyst maintain its original activity. In addition, Fig. S4 (ESI[†]) shows that hydrogen was produced steadily over the entire hour of our experiment.

In summary, we have proposed a new method to synthesize heterogeneous exposed core-shell catalyst arrays using space specificity, which was realized using an embodied micelle having two distinct regions to take different chemical sources. In addition, the structures and their formation mechanism of fabricated heterogeneous catalysts were also analysed using SEM, AFM, STEM, and TXRF. Furthermore, a heterogeneous Pt-TiO₂ catalyst array was also unveiled to allow a facile fabrication of efficient hydrogen generation *via* the photocatalytic water decomposition.

This work was supported by the Korea Center for Artificial Photosynthesis (KCAP) (NRF-2011-C1AAA001-2011-0030278), by the WCU program (R-31-2008-000-10055-0), by the Priority Research Centers Program (NRF-2011-0031407), National Research Foundation (NRF-2011-0028737), the Center for Inorganic Photovoltaic Materials (2012-0001174), the Hydrogen Energy R&D Center from a 21st Century Frontier R&D Program, and the Secondary Battery Program (NRF-2010-0029042).

Notes and references

- 1 A. T. Bell, *Science*, 2003, **299**, 1688.
- 2 M. A. Fox and M. T. Dulay, *Chem. Rev.*, 1993, **93**, 341.
- 3 S. Miao, Z. Liu, B. Han, J. Huang, Z. Sun, J. Zhang and T. Jiang, *Angew. Chem., Int. Ed.*, 2006, **45**, 266.
- 4 G. Palmisano, E. Garcia-Lopez, G. Marci, V. Loddo, S. Yurdakal, V. Augugliaro and L. Palmisano, *Chem. Commun.*, 2010, **46**, 7074.
- 5 M. Ni, M. K. H. Leung, D. Y. C. Leung and K. Sumathy, *Renewable Sustainable Energy Rev.*, 2007, **11**, 401.
- 6 G. Li, L. Lv, H. Fan, J. Ma, Y. Li, Y. Wan and X. S. Zhao, *J. Colloid Interface Sci.*, 2010, **348**, 342.
- 7 N. Lakshminarasimhan, W. Kim and W. Choi, *J. Phys. Chem. C*, 2008, **112**, 20451.
- 8 I. Sopyan, M. Watanabe, S. Murasawa, K. Hashimoto and A. Fujishima, *J. Photochem. Photobiol., A*, 1996, **98**, 79.
- 9 I. M. Arabatzis, T. Stergiopoulos, D. Andreeva, S. Kitova, S. G. Neophytides and P. Falaras, *J. Catal.*, 2003, **220**, 127.
- 10 P. Fu and P. Zhang, *Thin Solid Films*, 2011, **519**, 3480.
- 11 O. Akhavan, *J. Colloid Interface Sci.*, 2009, **336**, 117.
- 12 J. S. Jang, K. Y. Yoon, X. Xiao, F.-R. F. Fan and A. J. Bard, *Chem. Mater.*, 2009, **21**, 4803.
- 13 J. Eastoe, M. J. Hollamby and L. Hudson, *Adv. Colloid Interface Sci.*, 2006, **128-130**, 5.
- 14 F. Heshmatpour, R. Abazari and S. Balalaie, *Tetrahedron*, 2012, **68**, 3001.
- 15 N. Toshima and T. Yonezawa, *New J. Chem.*, 1998, **22**, 1179.
- 16 M. Aizawa and J. M. Buriak, *Chem. Mater.*, 2007, **19**, 5090.
- 17 Z. Zheng, B. Huang, X. Qin, X. Zhang, Y. Dai and M.-H. Whangbo, *J. Mater. Chem.*, 2011, **21**, 9079.
- 18 C.-H. Li, Y.-H. Hsieh, W.-T. Chiu, C.-C. Liu and C.-L. Kao, *Sep. Purif. Technol.*, 2007, **58**, 148.
- 19 X. Chen, S. Shen, L. Guo and S. S. Mao, *Chem. Rev.*, 2010, **110**, 6503.
- 20 A. Kudo and Y. Miseki, *Chem. Soc. Rev.*, 2009, **38**, 253.